JOC Article

Density Functional Study of the Ring Effect on the Myers−Saito Cyclization and a Comparison with the Bergman Cyclization

Wei-Chen Chen, Jian-Wei Zou, and Chin-Hui Yu*

Department of Chemistry, National Tsing Hua University, Hsinchu 300, Taiwan

chyu@oxygen.chem.nthu.edu.tw

Received November 15, 2002

Myers−Saito cyclizations of a series of enyne−allenes and enyne−butatrienes have been studied by density functional methods. The pure DFT method, BPW91, in conjunction with the 6-311** basis set is demonstrated to be suitable to study these systems. Geometry optimizations and harmonic frequency calculations were applied for every reactant, transition structure, as well as product. It has been shown that the cyclic structure of reactant lowers significantly the critical distance and reaction barrier. For the Myers−Saito product of (5Z)-1,2,3,5-cyclononatetraen-7-yne (**10R**), the confinement of ring leads to an essential change of the biradical character from $\sigma-\pi$ type to $\sigma-\sigma$ type. The through-bond coupling is therefore involved in this product as in the Bergman products. With the enlargement of the ring, the geometrical distortion weakens the through-bond coupling and raises the stability of the products. As a consequence, 1,5-didehydroindene (**10P**) presents a particularly long critical distance and lower thermodynamic stability. Detailed comparisons of the reactivities of **10R**, (*Z*)-1-cyclononene-3,8-diyne (**13R**), and (*Z*)-1-cyclodecene-3,9-diyne (**14R**) that represent the core structure of a category of natural antitumor drugs have also been made. It reveals that the reactivity of these three systems is quite similar, despite the fact that the thermochemical properties of the prototypical Myers−Saito and Bergman cyclizations are significantly different from each other.

Introduction

The cyclizations of enediynes and enyne−allenes, which are known as Bergman[1] and Myers−Saito[2] reactions, respectively, have recently received a lot of attention due to the discovery that these two reactions play a fundamental role in the biological activity of potent enediyne antitumor agents.[3] Naturally occurring examples of antitumor agents of this type are calicheamicin γ^{I}_{1} and neocarzinostatin.[4,5] The antitumor activity is attributed to the highly reactive Bergman or Myers−Saito biradical products. The biradicals are generally believed to be able to abstract two hydrogens from the deoxyribose sugar on both strands of the DNA, leading to the breakdown of the cancer chromosome.[3,6]

To provide insight into the Bergman and Myers−Saito reactions, as well as Schmittel reaction[7] that is found to compete with the Myers−Saito reaction, a number of theoretical studies have been devoted recently to investigate the prototypical reaction processes,[8−12] substituent effects,[13] benzannulation effects,[14] regioselectivity,[15] aromaticity,[16] and so forth. Moreover, computational efforts

(1) (a) Bergman, R. G. *Acc. Chem. Res.* **1973**, *6*, 25. (b) Jones, R. R.; Bergman, R. G. *J. Am. Chem. Soc.* **1972**, *94*, 660. (c) Lockhart, T. P.; Comita, P. B.; Bergman, R. G. *J. Am. Chem. Soc.* **1981**, *103*, 4082. (d) Lockhart, T. P.; Bergman, R. G. *J. Am. Chem. Soc.* **1981**, *103*, 4091.

(2) (a) Myers, A. G.; Kuo, E. Y.; Finney, N. S. *J. Am. Chem. Soc.* **1989**, *111*, 8057. (b) Myers, A. G.; Dragovich, P. S.; Kuo, E. Y. *J. Am. Chem. Soc.* **1992**, *114*, 9369. (c) Saito, I.; Watanabe, T.; Takahashi, K. *Chem. Lett.* **1989**, 2099. (d) Saito, I.; Nagata, R.; Yamanaka, H.; Murahashi, E. *Tetrahedron Lett.* **1990**, *31*, 2907. (e) Nagata, R.; Yamanaka, H.; Okazaki, E.; Saito, I. *Tetrahedron Lett.* **1989**, *30*, 4995.

(3) (a) Smith, A. L.; Nicolaou, K. C. *J. Med. Chem.* **1996**, *39*, 2103. (b) Nicolaou, K. C.; Dai, W.-M.; Tsay, S.-C.; Estevez, V. A.; Wrasidlo, W. *Science* **1992**, *256*, 1172. (c) Wang, K. K. *Chem. Rev.* **1996**, *96*, 207. (d) Nicolaou, K. C.; Smith, B. M.; Ajito, K.; Komatsu, H.; Gomez-Paloma, L.; Tor, Y. *J. Am. Chem. Soc.* **1996**, *118*, 2303.

(4) (a) Lee, M. D.; Dunne, T. S.; Siegel, M. M.; Chang, C. C.; Morton, G. O.; Borders, D. B. *J. Am. Chem. Soc.* **1987**, *109*, 3464. (b) Lee, M. D.; Dunne, T. S.; Chang, C. C.; Ellestad, G. A.; Siegel, M. M.; Morton, G. O.; McGahren, W. J.; Borders, D. B. *J. Am. Chem. Soc.* **1987**, *109*, 3466. (c) Lee, M. D.; Ellestad, G. A.; Borders, D. B. *Acc. Chem. Res.* **1992**, *24*, 235.

(5) (a) Myers, A. G. *Tetrahedron Lett.* **1987**, *28*, 4493. (b) Myers, A. G.; Proteau, P. J.; Handel, T. M. *J. Am. Chem. Soc.* **1988**, *110*, 7212.

(6) (a) Nicolaou, K. C.; Dai, W.-M. *Angew. Chem.* **1991**, *103*, 1453. (b) Takahashi, T.; Tanaka, H.; Yamada, H.; Matsumoto, T.; Sugiura, Y. *Angew. Chem., Int. Ed. Engl.* **1996**, *35*, 1835. (c) Nicolaou, K. C.; Smith, A. L.; Wendeborn, S. V.; Hwang, C.-K. *J. Am. Chem. Soc.* **1991**, *113*, 3106. (d) Nicolaou, K. C.; Li, T.; Nakada, M.; Hummel, C. W.; Hiatt, A.; Wrasidlo, W. *Angew. Chem., Int. Ed. Engl.* **1994**, *33*, 183.

(7) (a) Schmittel, M.; Strittmatter, M.; Kiau, S. *Angew. Chem.* **1996**, *108*, 1952. (b) Schmittel, M.; Kiau, S.; Siebert, T.; Strittmatter, M. *Tetrahedron Lett.* **1996**, *37*, 7691. (c) Schmittel, M.; Steffen, J.-P.; Auer, D.; Maywald, M. *Tetrahedron Lett.* **1997**, *38*, 6177. (d) Schmittel, M.; Keller, M.; Kiau, S.; Strittmatter, M. *Chem. Eur. J.* **1997**, *3*, 807. (e) Schmittel, M.; Strittmatter, M.; Kiau, S. *Tetrahedron Lett.* **1995**, *36*, 4975.

(8) (a) Lindh, R.; Lee, T. J.; Bernhardsson, A.; Persson, B. J.; Karlstrom, G. *J. Am. Chem. Soc.* **1995**, *117*, 7186. (b) Lindh, R.; Persson, B. J. *J. Am. Chem. Soc.* **1994**, *116*, 4963.

(9) (a) Schreiner, P. R.; Prall, M. *J. Am. Chem. Soc.* **1999**, *121*, 8615. (b) Schreiner, P. R. *J. Am. Chem. Soc.* **1998**, *120*, 4184.

(10) (a) de Visser, S. P.; Filatov, M.; Shaik, S. *Phys. Chem. Chem. Phys.* **2001**, *3*, 1242. (b) Engels, B.; Hanrath, M. *J. Am. Chem. Soc.* **1998**, *120*, 6356.

(11) McMahon, R. J.; Halter, R. J.; Fimmen, R. L.; Wilson, R. J.; Peebles, S. A.; Kuczkowski, R. L.; Stanton, J. F. *J. Am. Chem. Soc.* **2000**, *122*, 939.

(12) (a) Cramer, C. J. *J. Am. Chem. Soc.* **1998**, *120*, 6261. (b) Kraka, E.; Cremer, D. *J. Am. Chem. Soc.* **1994**, *116*, 4929.

10.1021/jo0267246 CCC: $25.00
Published on Web 04/09/2003

aimed at designing new enediyne antitumor drugs with good selectivity have also been reported[17] because those natural products cleave the DNA of normal cells, limiting their merit. Nevertheless, the *warhead* of natural enediyne antitumor drugs is a cyclic structure instead of an open-end one that most model compounds in previous studies used. Ring strain, as several authors pointed out,[9,18−20] has a large effect on both the Bergman and Myers−Saito reactions. In turn, the strain provides a way of facilitating the synthesis of other enediyne drugs. In one of our previous studies,[20] we have investigated the ring effects on the Bergman reaction by using the DFT method and found that the critical distance, which is the distance between the two atoms that form a new bond during cyclization, and the energetic are affected substantially by the ring size, the substitution, and the conformational structure.

Although similarity exists, the prototypical Myers−Saito reaction differs from the prototypical Bergman reaction at least in the following two aspects: first, Myers−Saito cyclization gives rise to a $\sigma-\pi$ biradical while Bergman cyclization produces a $\sigma-\sigma$ biradical; second, Myers−Saito cyclization is thought to be exothermic, while Bergman cyclization is endothermic. Thus, the ring effects on these two cyclizations may be expected to be different in some aspects. This is supported indirectly by a recent study by Schreiner and Prall,[9a] who studied in parallel the Myers−Saito and Schmittel cyclizations by using the DFT method. Additionally, one has to bear in mind that the reactants of the Myers−Saito cyclization for naturally occurring antitumor agents, such as neocarzinostatin, are enyne−butatrienes rather than enyne−allenes. In comparison with the biradical product of enyne−allene, which is solely of the $\sigma-\pi$ type, the product of enyne−butatriene exhibits two possible structures (Scheme 1): **A**, $\sigma-\pi$ biradical, i.e., the exocyclic radical site located in the 2p orbital, and **B**, $\sigma-\sigma$ biradical, i.e., the exocyclic radical site located in the sp^2 orbital. Accordingly, the ring effect on these two systems should be different.

The goal of this work is to further explore how the ring strain influences the Myers−Saito cyclizations. For this purpose, reactions of the following systems: (4*Z*)-1,2,4-heptatrien-6-yne (**1R**), (3*Z*)-3,5,6-octatrien-1-yne (**2R**), (4*Z*)-1,2,4-octatrien-6-yne (**3R**), (5*Z*)-2,3,5-nonatrien-7-yne (**4R**), (4*Z*)-1,2,4-cyclononatrien-6-yne (**5R**), (4*Z*)-1,2,4-cyclodecatrien-6-yne (**6R**), (4*Z*)-1,2,4-cycloundecatrien-6-yne (**7R**), (5*Z*)-1,2,3,5-octatetraen-7-yne (**8R**), (5*Z*)-1,2,3,5-nonatetraen-7-yne (**9R**), (5*Z*)-1,2,3,5-cyclononatetraen-7-yne (**10R**), (5*Z*)-1,2,3,5-cyclodecatetraen-7-yne (**11R**), and (5*Z*)-1,2,3,5-cycloundecatetraen-7-yne (**12R**), as shown in Chart 1, where **1R** through **7R** belong to the enyne−allene family and **8R**−**12R** belong to the enyne−butatriene family, are examined. For the sake of convenience, here and throughout this paper, ***n***, ***n*R**, ***n*TS**, and ***n*P** are used to denote the number of reactions, the corresponding reactants, transition states and products, respectively. The compound **10R**, together with two Bergman reactants investigated previously,[20] (*Z*)-1-cyclononene-3,8-diyne (**13R**) and (*Z*)-1-cyclodecene-3,9-diyne (**14R**), as illustrated in Chart 2, are the core structures of three different natural enediyne antitumor drugs, indicating the similarity among these three systems. Thus, comparisons of ring effects on the Myers−Saito cyclizations with those on the Bergman cyclizations are of interest and also investigated in the present paper. High-level *ab initio* calculations that include substantial electron correlation, although of significance for biradical species, are not feasible for these systems. The DFT method is proven to be an ideal alternative by numerous recent studies.[9,10,12a,17c,20−25] In this paper, we report the geometries and frequencies at each optimized structure of reaction **1**−**12** and intrinsic reaction coordinate (IRC) calculations carried out with density functional methods; energies and thermodynamic data deduced from the calculations are also displayed. The data provide a base for the discussion of the mechanism of the Myers−Saito reaction.

SCHEME 1

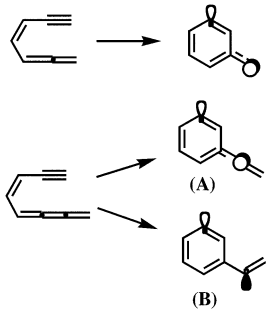

Computational Details

The pure density functional method, BPW91,[26,27] in conjunction with the 6-311G** basis set, was employed to study the Myers−Saito reaction of **1**−**12**. The structures of reactants, transition structures (TS), and products were fully optimized without any constraints. All stationary structures were identified at minima for reactants and products, which had no imaginary frequency, or at saddle points for TS, which had one and only one imaginary frequency with the vibration mode

(13) (a) Prall, M.; Wittkopp, A.; Fokin, A. A.; Schreiner, P. R. *J. Comput. Chem.* **2001**, *22*, 1605. (b) Plourde, G. W., II; Warner, P. M.; Parrish, D. A.; Jones, G. B. *J. Org. Chem.* **2002**, *67*, 5369. (c) Jones, G. B.; Warner, P. M. *J. Am. Chem. Soc.* **2001**, *123*, 2134.
(14) (a) Wenthold, P. G.; Lipton, M. A. *J. Am. Chem. Soc.* **2000**, *122*, 9265. (b) Prall, M.; Wittkopp, A.; Schreiner, P. R. *J. Phys. Chem. A* **2001**, *105*, 9265. (c) Koseki, S.; Fujimura, Y.; Hirama, M. *J. Phys. Chem. A* **1999,** *103*, 7672.
(15) Musch, P. W.; Remenyi, C.; Helten. H.; Engels, B. *J. Am. Chem. Soc.* **2002**, *124*, 1823.
(16) Stahl, F.; Moran, D.; Schleyer, P. R.; Prall, M.; Schreiner, P. R. *J. Org. Chem.* **2002**, *67*, 1453.
(17) Kraka, E.; Cremer, D. *J. Am. Chem. Soc.* **2000**, *122*, 8245. (b) Kraka, E.; Cremer, D. *J. Comput. Chem.* **2001**, *22*, 216. (c) Feldgus, S.; Shields, G. C. *Chem. Phys. Lett.* **2001**, *347*, 505.
(18) Schreiner, P. R. *J. Chem. Soc., Chem. Commun.* **1998**, 483.
(19) Schmittel, M.; Steffen, J. P.; Maywald, M.; Engels, B.; Helten, H.; Musch, P. *J. Chem. Soc., Perkin Trans. 2* **2001**, 1331.
(20) Chen, W.-C.; Chang, N.-Y.; Yu, C.-H. *J. Phys. Chem. A* **1998**, *102*, 2584.
(21) Cramer, C. J.; Nash, J. J.; Squires R. R. *Chem. Phys. Lett.* **1997**, *277*, 311.
(22) Cramer, C. J.; Squires, R. R. *J. Phys. Chem. A* **1997**, *101*, 9191.
(23) Lim, M. H.; Worthington, S. E.; Dulles, F. J.; Cramer, C. J. *Density Functional Calculations of Radicals and Diradicals*; in *Density-Functional Methods in Chemistry*; Laird, B. B., Ross, R. B., Ziegler, T., Eds.; American Chemical Society: Washington, DC, 1996; p 402.
(24) Prall, M.; Kruger, A.; Schreiner, P. R.; Hopf, H. *Chem. Eur. J.* **2001**, *7*, 4386.
(25) De Proft, F.; Schleyer, P. v. R.; van Lenthe, J. H.; Stahl, F.; Geerlings, P. *Chem. Eur. J.* **2002**, *8*, 3402
(26) Becke, A. D. *Phys. Rev. A* **1988**, *38*, 3098.
(27) Perdew, J. P.; Wang, Y. *Phys. Rev. B* **1992**, *45*, 13244.

CHART 1

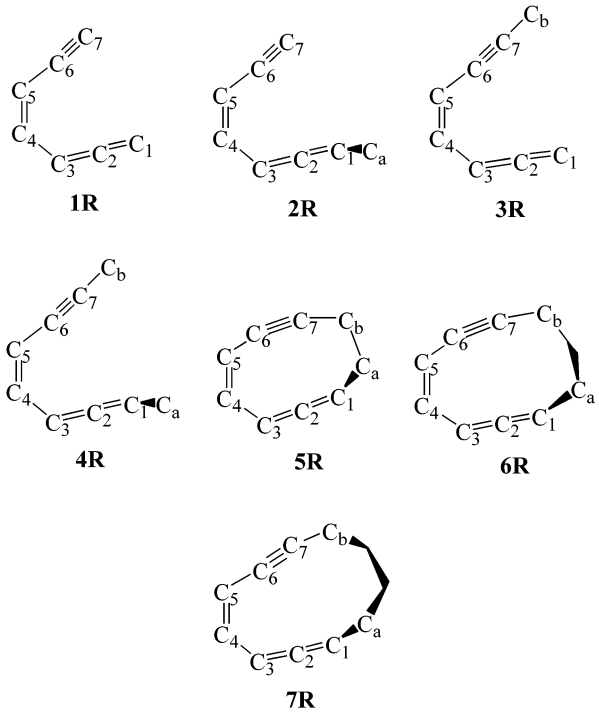

(a) Enyne-allenes

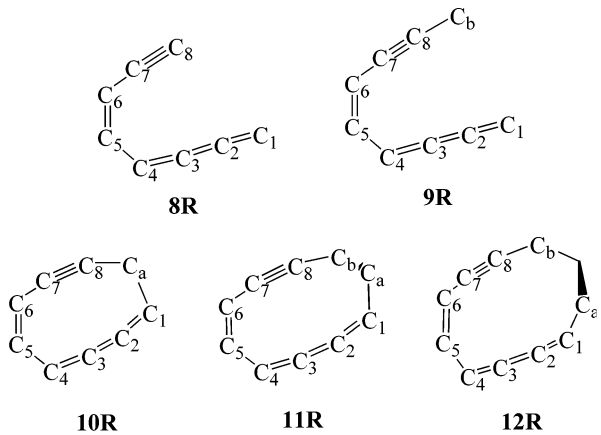

(b) Enyne-trienes

CHART 2

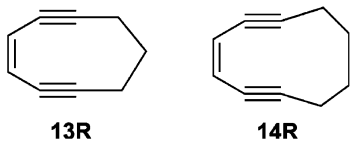

corresponding to the reaction coordinate. Thermodynamic data, such as Gibbs free energy (ΔG), Gibbs activation free energy ($\Delta G^{\ddagger}$), reaction entropy (ΔS), and activation entropy ($\Delta S^{\ddagger}$) of each reaction were calculated using the canonical ensemble sampling of the vibrational and rotational modes at several temperatures.

The prototypical Myers−Saito reaction **1**, the cyclization to form the singlet α,3-didehydrotoluene (**1P**), was also studied with several other density functional methods, including BP86,[26,28] BLYP,[26,29] and the hybrid B3LYP,[29,30] in conjunction with the 6-311G** basis set. Single-point energies of all stationary structures of reaction **1** optimized with aforementioned DFT methods were evaluated by using the coupled-cluster with single and double excitations of full electrons plus perturbatively included triplet excitations, CCSD(T)[31,32] and BCCD(T),[33,34] which is the CCSD(T) calculation benefit from using Brueckner-type orbitals, methods with the 6-31G** basis set. Multi-configuration calculations, MCSCF and MRCI, were also carried out. For all reactions, the restricted calculations were employed for the reactant and the transition structure. For the biradical product, the unrestricted density functional methods were utilized and the coupled cluster calculations were applied with the unrestricted SCF orbitals. The justification of the choice of computational methods is interpreted in the Discussion.

The IRC calculation was utilized to study the relationship of the energy profiles of reactions **1** and **10** against the critical distance. To understand the similarity in reactivity between Myers−Saito reactant **10R** and Bergman reactants **13R** and **14R**, a comparison of the energy profile for reaction **10** with those for reactions **13** and **14** given in our previous study[20] was made. Thermodynamic data ΔG, $\Delta G^{\ddagger}$, ΔH, $\Delta H^{\ddagger}$, ΔS, and $\Delta S^{\ddagger}$ of these three reactions were also computed to explore their resemblance.

The DFT and IRC calculations were performed with Gaussian 98[35] using SGI Origin 2000, HP SPP2000, and Fujitsu VPP300 workstations. Couple-cluster methods were carried out with ACES II[36] on the Compaq Alpha workstation. Multiconfiguration computations, MCSCF and MRCI, were executed on the same platforms by the MOLPRO 98 program.[37]

Results

The Structure of Product. The C_2-C_7 cyclization of **1R** represents the prototypical Myers−Saito reaction. A relationship of the energies obtained from the IRC calculation against the critical distance, R_{C2C7}, is plotted as the solid line in Figure 1a. The product obtained from the IRC calculation (**1P′**), however, is not the one we need. Upon examining the structure of **1P′**, we found that this species possesses a distorted benzene ring with a distortion angle approximately 20° as depicted in Figure

(28) Perdew, J. P. *Phys. Rev. B* **1986**, *33*, 8822.
(29) Lee, C.; Yang, W.; Parr, R. G. *Phys. Rev. B* **1988**, *37*, 785.
(30) Becke, A. D. *J. Chem. Phys.* **1993**, *98*, 5648.
(31) Scuseria, G. E. *Chem. Phys. Lett.* **1991**, *176*, 27.
(32) Bartlett, R. J.; Watts, J. D.; Kucharski, S. A.; Noga, J. *Chem. Phys. Lett.* **1990**, *165*, 513.
(33) Brueckner, K. A. *Phys. Rev.* **1954**, *96*, 508.
(34) (a) Scuseria, G. E. *Chem. Phys. Lett.* **1994**, *226*, 251. (b) Scuseria, G. E.; Schaefer, H. F., III. *Chem. Phys. Lett.* **1987**, *142*, 354.
(35) Frisch, M. J.; Trucks, G. W.; Schlegel, H. B.; Scuseria, G. E.; Robb, M. A.; Cheeseman, J. R.; Zakrzewski, V. G.; Montgomery, J. A., Jr.; Stratmann, R. E.; Burant, J. C.; Dapprich, S.; Millam, J. M.; Daniels, A. D.; Kudin, K. N.; Strain, M. C.; Farkas, O.; Tomasi, J.; Barone, V.; Cossi, M.; Cammi, R.; Mennucci, B.; Pomelli, C.; Adamo, C.; Clifford, S.; Ochterski, J.; Petersson, G. A.; Ayala, P. Y.; Cui, Q.; Morokuma, K.; Malick, D. K.; Rabuck, A. D.; Raghavachari, K.; Foresman, J. B.; Cioslowski, J.; Ortiz, J. V.; Stefanov, B. B.; Liu, G.; Liashenko, A.; Piskorz, P.; Komaromi, I.; Gomperts, R.; Martin, R. L.; Fox, D. J.; Keith, T.; Al-Laham, M. A.; Peng, C. Y.; Nanayakkara, A.; Gonzalez, C.; Challacombe, M.; Gill, P. M. W.; Johnson, B. G.; Chen, W.; Wong, M. W.; Andres, J. L.; Head-Gordon, M.; Replogle, E. S.; Pople, J. A. *Gaussian 98*, revision A.7; Gaussian, Inc.: Pittsburgh, PA, 1998.
(36) ACES II: Stanton, J. F.; Gauss, J.; Watts, J. D.; Lauderdale, W. J.; Bartlett, R. J. *Int. J. Quantum Chem. Symp.* **1992**, *26*, 879.
(37) MOLPRO is a package of ab initio programs written by Werner, H.-J. and Knowles, P. J. with contributions from Amos, R. D.; Celani, P.; Cooper, D. L.; Deegan, M. J. O.; Dobbyn, A. J.; Eckert, F.; Hampel, C.; Hetzer, G.; Korona, T.; Lindh, R.; Lloyd, A. W.; McNicholas, S. J.; Manby, F. R.; Meyer, W.; Mura, M. E.; Nicklass, A.; Palmieri, P.; Pitzer, R.; Rauhut, G.; Schutz, M.; Stoll, H.; Stone, A. J.; Tarroni, R.; Thorsteinsson, T.

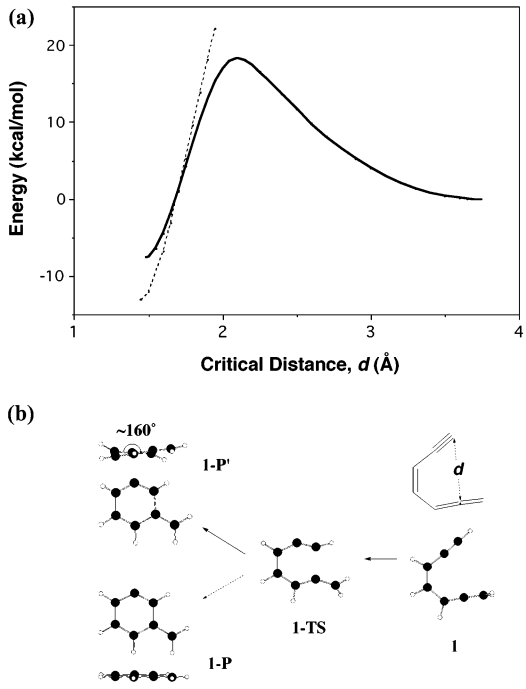

FIGURE 1. (a) Energetic profile of prototypical Myers−Saito reaction **1**. (b) Ground-state product (**1P**) and excited-state product (**1P′**).

1b and represents a closed-shell electronic configuration. In the ground state of **1P**, which is lower in energy than **1P′** by about 5 kcal/mol, the two unpaired electrons are located in different radical orbitals, and all atoms are coplanar. A plot of the energies of **1P** versus the critical distance, the dashed line in Figure 1a, shows that this curve will intersect with the potential energy curve of **1P′**. Thus, **1P** is the true product of the prototypical Myers−Saito reaction.

Geometry. The optimized geometries of enyne−allenes **1R**−**7R**, their transition structures for Myers−Saito cyclizations, as well as the corresponding biradical products are listed in Tables S1−S3 (Supporting Information). Tables S4−S6 (Supporting Information) list those of enyne−butatrienes **8R**−**12R**, where the atom labeling for each species is given in Chart 1.

The critical distances of **1TS** through **7TS**, R_{C2C7}, are all approximately 2.1 Å, while those of **8TS** through **12TS**, R_{C3C8}, are 2.040, 2.041, 1.940, 2.016, and 2.024 Å, respectively. Each transition structure is characterized by one and only one imaginary frequency, which is found to range from 425i to 470i. Normal-mode analysis clearly indicates that the imaginary frequency mode corresponding to the reaction coordinate is the C−C stretching between the two carbon atoms forming the new bond. From the small differences in critical distance and vibrational frequency among these transition states, one would anticipate that the curvatures of potential energy surfaces where these transition structures locate are quite similar. Therefore, the cyclization barriers and reverse barriers for these reactions are mainly determined by the thermodynamic stabilities of the corresponding reactants and products.

For cyclic reactants **5R**, **6R**, and **7R**, the critical distance which is confined by the ring to be 2.969, 3.238, and 3.418 Å, respectively, is considerably shorter than 3.7 Å of **1R**−**4R**. This shortening results in the lowering of stability and the elevating of reactivity for cyclic reactants. Similar results are also observed in enyne−butatriene systems. The angles $\angle C_1C_2C_3$ in **10P**−**12P** are 116.6°, 129.7°, and 144.4°, respectively, differing remarkably from that being ∼180.0° in **8P** and **9P** due to the confinement of cyclic structures. Moreover, the space confinement causes the C_2 radical centers to be located at the hybrid sp^2 orbitals, **A** of Scheme 1, in **10P**−**12P**, rather than at *2*p orbitals, **B** of Scheme 1, as in **8P** and **9P**.

Energy. The energies of the Myers−Saito reactions **1**−**12** without zero-point energy (ZPE) correction, including the energies of reactants, transition states, and products, are summarized in Table 1. As can be seen from Table 1, the barriers for reactions **1**−**12** range from 13.69 to 20.63 kcal/mol, while the reaction energies range from −15.50 to −4.17 kcal/mol for enyne−allene systems and from −4.46 to 9.07 kcal/mol for enyne−butatriene systems. The energy released by the Myers−Saito cyclizations for enyne−butatriene systems is considerably smaller than that for enyne−allene systems. The cyclization does not lower, but rather raises the energy of **10P**. The reverse barriers for enyne−allene systems are all higher than 24.8 kcal/mol, while those for enyne−butatriene systems are all lower than 22.3 kcal/mol. For instance, the reverse barrier height of reaction **10** is as low as merely 7.26 kcal/mol, indicating that the products **8P**−**12P** are less stable. When zero-point energies are incorporated in the calculations of energies, the reaction energies increase while the reaction barriers decrease, but most of them vary within 1.0 kcal/mol, as shown in Table 2. Also listed in Table 2 are thermodynamic data calculated at 298.15, 373.15, and 500.00 K. The data at other temperatures, 273.15, 310.65, 423.15, and 473.15K, are provided as Supporting Information, given in Table S7. The activation free energies ($\Delta G^{\ddagger}$) calculated at 298.15 K are generally higher than 18 kcal/mol for acyclic systems and even higher than 22 kcal/mol for the methyl substituent systems **3**, **4**, and **9**. Nevertheless, for cyclic systems, the $\Delta G^{\ddagger}$ values are lower than 17 kcal/mol. This indicates clearly that the methyl substituent retards the Myers−Saito cyclization, whereas the ring strain effect facilitates the reaction.

Discussion

The Choice of Computation Method. Although it has been demonstrated by several groups[9,18,20−23] that pure DFT methods are suitable for describing the reaction involving biradical species, the BPW91, BP86, BLYP, as well as B3LYP methods in conjunction with the 6-311G** basis set are employed to study the prototipical Myers-Saito reaction, reaction 1, to ensure that the BPW91 method selected by us in a previous study[20] to investigate the ring effects of Bergman reactions is also suitable for the present purpose. The results are compared with the single-point calculations by CCSD, CCSD(T), BCCD, and BCCD(T) and are shown in Table 3. It has been demonstrated previously[9a] that the consideration of triple excitation in CC or BCC significantly lower

TABLE 1. Energies of Reactants, Transition States, and Products of Reactions 1−12 Obtained with BPW91/6-311G [a]**

1R	2R		3R		4R		5R	6R	7R	8R	9R	10R	11R	12R
−270.23472	−309.55499		−309.56275		−348.88256		−347.66690	−386.98682	−426.30441	−308.31924	−347.64763	−346.43480	−385.75323	−425.07365
1TS	**2TS$_1$**	**2TS$_2$**	**3TS**		**4TS$_1$**	**4TS$_2$**	**5TS**	**6TS**	**7TS**	**8TS**	**9TS**	**10TS**	**11TS**	**12TS**
18.34	17.54	17.98	19.81		20.63	19.73	13.69	14.06	16.50	17.81	19.93	16.34	14.35	16.36
1P	**2P$_1$**	**2P$_2$**	**3P**		**4P$_1$**	**4P$_2$**	**5P**	**6P**	**7P**	**8P**	**9P**	**10P**	**11P**	**12P**
−13.05	−13.15	−12.98	−7.62		−4.17	−7.42	−14.74	−15.50	−8.58	−4.46	0.45	9.07	−0.96	0.82

[a] Absolute energies of reactants are given in hartrees; others relative to the reactants are given in kcal/mol.

the activation energy of reaction **1**, and the computed values are closer to the experimental result.[2b] Thus, the experimental results, as well as the data calculated at CCSD(T) and BCCD(T) levels of theory will be used as references for selecting computational methods. As can be noted from Table 3, pure DFT funtionals, such as BPW91, BP86, and BLYP, yield a lower barrier than the hybrid B3LYP method. The barrier calculated by the BLYP method is closer to the reference value than those by others. For BPW91, BP86, and B3LYP methods, the calculated reaction energies are −13.05, −12.50, and −11.87 kcal/mol, respectively, close to the reference energies calculated by the CCSD(T) and BCCD(T) methods. However, the reaction energy obtained by BLYP is −5.78 kcal/mol, which is significantly lower than the reference reaction energies. Schreiner and Prall[9a] showed recently that BLYP and BPW91 with 6-31G* basis sets are quite suitable to describe the Myers−Saito and Schmittel cyclizations, and they preferred BLYP because it provided a more reliable reaction barrier. However, judging from the reaction energy, both presented in this work and the literature, the BLYP method may not be an optimal choice.

It seems that the B3LYP calculation can roughly describe this system. Engels and Hanrath,[10b] who used the CASSCF(10,10), MR-CI+Q,[38] and B3LYP methods to study the prototypical reaction **1**, then qualified the B3LYP as the DFT method of choice. Nevertheless, a recent theoretical study showed that some unusual problems were encountered when this method was used. Moreover, the hybrid DFT method, B3LYP, has been proven by several groups[9,18,20−23] to be unsuitable for studying the similar Bergman reaction. Thus, this method is also relinquished in the present study. The results calculated with the other two pure DFT functionals, BPW91 and BP86, are very close to each other, both reproduce the reference energies, especially the reaction energy well, and BPW91 gives slightly better results. With these comparisons in hand, and in order to be comparable with the previous results of the study of the Bergman reaction, we selected BPW91 with the 6-311G** basis set as the computational method in this work.

The reliability of the single determinant referenced couple cluster method was checked by the T1 diagnostic[39] of CCSD(T) calculations for the transition state and the biradical product, and the T1 values are 0.0120 and 0.0207, respectively. Conventionally, these values indicate that the single determinant method can be applied to the systems; in particular, the very small T1 of the transition state hints that it is somewhat close to a closed-shell nature. The validity of the UDFT to the biradical product requires justification because some problems of conventional Kohn−Sham DFT, such as orbital instability in conjunction with biradicals, have been noticed recently.[40] Nevertheless, for the prototipical

(38) (a) Eade, R. H. E.; Robb, M. A. *Chem. Phys. Lett.* **1981**, *83*, 362. (b) Hegarty, D.; Robb, M. A. *Mol. Phys.* **1979**, *38*, 1795. (c) Squires, R. R.; Cramer, C. J. *J. Phys. Chem. A* **1998**, *102*, 9072. (d) Malmqvist, P.-A.; Roos, B. O. *Chem. Phys. Lett.* **1989**, *155*, 189.

(39) Lee, T. J.; Taylor P. R. *Int. J. Quantum Chem. Symp.* **1989**, *23*, 199.

(40) (a) Gräfenstein, J.; Hjerpe, A. M.; Kraka, E.; Cremer, D. *J. Phys. Chem. A* **2000**, *104*, 1748. (b) Crawford, T. D.; Kraka, E.; Stanton, J. F.; Cremer, D. *J. Chem. Phys.* **2001**, *114*, 10638. (c) Gräfenstein, J.; Kraka, E.; Filatov, M.; Cremer, D. *Int. J. Mol. Sci.* **2002**, *3*, 360. (d) Krylov, A. I.; Sherrill, C. D. *J. Chem. Phys.* **2002**, *116*, 3194.

TABLE 2. Reaction Energies (ΔE) and Reaction Barriers ($\Delta E^{\ddagger}$) with the ZPE Correction, Enthalpies, Entropies, Free Energies of Reaction (ΔH, ΔS, and ΔG), and Activation Enthalpies, Activation Entropies, and Activation Free Energies ($\Delta H^{\ddagger}$, $\Delta S^{\ddagger}$, and $\Delta G^{\ddagger}$) of Systems 1−12 (Energies in kcal/mol and Entropies in cal K^{-1} mol^{-1})

	1	**2_1**	**2_2**	**3**	**4_1**	**4_2**	**5**	**6**	**7**	**8**	**9**	**10**	**11**	**12**
							Relative Energy with the ZPE Correction							
$\Delta E^{\ddagger}$	18.20	17.26	17.77	19.68	20.41	19.51	12.83	13.38	16.03	17.35	19.67	15.76	13.81	15.83
ΔE	−11.45	−11.96	−11.77	−6.25	−3.04	−6.38	−14.67	−14.98	−7.90	−3.74	0.82	9.28	−0.10	1.48
							298.15 K							
ΔH	−12.57	−12.87	−12.66	−7.51	−4.24	−7.48	−15.10	−15.68	−8.63	−4.49	0.00	8.72	−0.90	0.65
ΔS	−10.58	−7.66	−4.62	−13.86	−13.66	−12.47	−2.05	−4.93	−5.32	−6.14	−8.22	−3.81	−5.40	−6.13
ΔG	−9.42	−10.59	−11.28	−3.37	−0.17	−3.76	−14.49	−14.21	−7.05	−2.66	2.46	9.85	0.71	2.48
$\Delta H^{\ddagger}$	17.37	16.45	16.98	18.66	19.40	18.55	12.42	12.84	15.36	16.70	18.70	15.23	13.21	15.15
$\Delta S^{\ddagger}$	−8.43	−8.32	−7.98	−12.10	−12.58	−11.88	−2.60	−3.81	−5.06	−5.81	−11.27	−3.45	−3.82	−5.32
$\Delta G^{\ddagger}$	19.88	18.94	19.36	22.27	23.16	22.09	13.20	13.97	16.86	18.43	22.06	16.26	14.35	16.73
							373.15 K							
ΔH	−12.83	−13.12	−12.91	−7.70	−4.43	−7.66	−14.31	−15.86	−8.81	−4.72	−0.16	8.57	−1.11	0.45
ΔS	−11.36	−8.40	−5.38	−14.45	−14.23	−13.03	−2.48	−5.47	−5.86	−6.82	−8.72	−4.24	−6.04	−6.74
ΔG	−8.59	−9.99	−10.90	−2.31	0.88	−2.80	−15.24	−13.82	−6.63	−2.17	3.09	10.16	1.14	2.96
$\Delta H^{\ddagger}$	17.16	16.25	16.77	18.48	19.22	18.36	12.28	12.67	15.18	16.50	18.51	15.05	13.03	14.96
$\Delta S^{\ddagger}$	−9.04	−8.93	−8.61	−12.65	−13.13	−12.44	−3.03	−4.31	−5.60	−6.42	−11.84	−3.99	−4.38	−5.89
$\Delta G^{\ddagger}$	20.54	19.58	19.98	23.20	24.12	23.00	13.41	14.28	17.27	18.89	22.93	16.54	14.66	17.16
							500.00 K							
ΔH	−13.14	−13.41	−13.22	−7.90	−4.63	−7.85	−15.39	−16.04	−9.01	−4.99	−0.32	8.43	−1.34	0.23
ΔS	−12.07	−9.09	−6.09	−14.91	−14.69	−13.48	−2.82	−5.90	−6.31	−7.45	−9.10	−4.57	−6.57	−7.24
ΔG	−7.10	−8.87	−10.17	−0.44	2.72	−1.11	−13.97	−13.09	−5.85	−1.26	4.23	10.72	1.95	3.85
$\Delta H^{\ddagger}$	16.86	15.95	16.46	18.21	18.96	18.09	12.04	12.42	14.91	16.19	18.24	14.78	12.75	14.68
$\Delta S^{\ddagger}$	−9.74	−9.62	−9.32	−13.26	−13.74	−13.06	−3.57	−4.89	−6.23	−7.13	−12.47	−4.62	−5.01	−6.54
$\Delta G^{\ddagger}$	21.73	20.76	21.12	24.85	25.83	24.62	13.83	14.87	18.02	19.76	24.48	17.09	15.26	17.95

TABLE 3. Comparison of Total Energies (E_{tot}), Activation Energy ($\Delta E^{\ddagger}$), and Reaction Energy (ΔE) for Prototypical Myers−Saito Cyclization at Various Levels of Theory (Total Energies in Hartrees, Other Energies in kcal/mol)

	E_{tot}	$\Delta E^{\ddagger}$	ΔE
BPW91/6-311G**// BPW91/6-311G**	−270.234717	18.34	−13.05
UCCSD/6-31G**// BPW91/6-311G**	−269.418245	27.01	−15.27
UCCSD(T)/6-31G**// BPW91/6-311G**	−269.463039	21.82	−12.06
UBCCD/6-31G**// BPW91/6-311G**	−269.416070	27.09	−16.07
UBCCD(T)/6-31G**// BPW91/6-311G**	−269.463257	21.77	−13.76
BP86/6-311G**// BP86/6-311G**	−270.265233	17.68	−12.50
UCCSD/6-31G**// BP86/6-311G**	−269.418137	27.06	−15.16
UCCSD(T)/6-31G**// BP86/6-311G**	−269.463052	21.87	−11.92
UBCCD/6-31G**// BP86/6-311G**	−269.415952	27.14	−15.96
UBCCD(T)/6-31G**// BP86/6-311G**	−269.463271	21.82	−13.63
BLYP/6-311G**// BLYP /6-311G**	−270.165047	21.20	−5.78
UCCSD/6-31G**// BLYP /6-311G**	−269.418231	27.68	−15.09
UCCSD(T)/6-31G**// BLYP /6-311G**	−269.463050	22.00	−11.92
UBCCD/6-31G**// BLYP /6-311G**	−269.416047	27.76	−15.87
UBCCD(T)/6-31G**// BLYP /6-311G**	−269.463268	21.95	−13.65
B3LYP/6-311G**// B3LYP /6-311G**	−270.277191	24.65	−11.87
UCCSD/6-31G**// B3LYP /6-311G**	−269.418651	28.01	−15.31
UCCSD(T)/6-31G**// B3LYP /6-311G**	−269.462635	22.26	−12.44
UBCCD/6-31G**// B3LYP /6-311G**	−269.416550	28.06	−16.06
UBCCD(T)/6-31G**// B3LYP /6-311G**	−269.462846	22.21	−14.06
CASSCF(10,10)[a,b]	−268.577620	29.00	4.00
MRCI+Q// CASSCF(10,10)[a,b]	−269.327850	25.00	−21.00
B3LYP/6-31G* [a]	−270.201690	22.00	−17.00
BPW91/6-31G* [c]		18.00	−13.80
BLYP/6−31 G* [c]		20.20	−7.80
BPW91/cc-pVTZ// BPW91/6-31G* [c]		19.60	−9.40
BLYP/cc-pVTZ// BLYP/6-31G* [c]		22.70	−2.10
CCSD(T)/cc-pVDZ// BLYP/6-31G* [c]		22.20	−24.30
BCCD(T)/cc-pVDZ// BLYP/6-31G* [c]		22.20	−11.90
REKS−BLYP/6-31G* [d]		22.0	−8.3
Experiment[e]		22 ± 1	−15 ± 3

[a] Reference 10b. [b] For carbon, a Huzinaga's (9s5p) AO basis set in the Dunning [4s2p] contraction with *d*-functions added; for hydrogen, a Huzinaga's (4s) AO basis set in the Dunning [2s] contraction. [c] Reference 9a. [d] Reference 10a. [e] Reference 2b.

Myers-Saito reaction, the current calculated BPW91/6-311G** reaction energy is not at all inferior to a previous result[10a] predicted by the spin-restricted ensemble-referenced Kohn−Sham (PEKS) method, which has been found to be quite suitable for studies of biradical systems.[41] Several recent studies also applied the KS-DFT to biradical systems without encountering difficulties.

Structures Involved in the Myers−Saito Reactions. The critical distances R_{C2C7} of cyclic enyne−allene reactants **5R**, **6R**, and **7R** are 2.969, 3.238, and 3.418 Å, respectively, differing distinctly from those of acyclic **1R**−**4R**, which are about 3.7 Å. Several bond angles and dihedral angles are also distorted due to the cyclic structure. However, the bond angle $\angle C_1C_2C_3$, which keeps linearity ∼176° in all enyne−allene reactants, is almost not influenced by the ring structure due to the allenic bonding of these three atoms. In **2R** and **4R**, the C_a atom bonded to C_1 through a σ bond, which is out of the plane formed by the other carbon atoms. However, in the cyclic reactants **5R**, **6R**, and **7R**, this atom has to connect with the two neighboring carbon atoms simultaneously, so the ring strain comes into being. The strain can be partially released by distorting the dihedral angle of the two allenic planes that are orthogonal in acyclic systems. The dihedral angle of $\varphi_{CaC1C3C4}$ is 71.6° in **5R**, 81.7° in **6R**, and 82.7° in **7R**. Another dihedral angle $\varphi_{C2C3C4C5}$ is also affected by the strain effects and distorted about 22° in these reactants. As a consequence, the cyclic reactants become less stable, and the reaction barriers for Myers−Saito reactions decrease. As the Myers−Saito cyclization proceeds, a new bond will be formed between the C_2 and C_7 atoms, and C_2−C_7 will form an aromatic ring. On the other hand, the π bond of C_1═C_2 will be broken, and the 2p orbital of C_2 will be rotated to stabilize the benzylic radical. The C_1C_2 bond is rotated by 30−35° in all transition structures of ene−allenes **1TS**−**7TS**.

(41) (a) Filatov, M.; Shaik, S. *Chem. Phys. Lett.* **1999**, *304*, 429. (b) Filatov, M.; Shaik, S. *J. Phys. Chem. A* **2000**, *104*, 6628.

The critical distances of **1TS**−**7TS** are about 2.1 Å, and the only imaginary frequency of them is between 429i and 470i. The products **1P**−**7P** maintain the aromatic plane, except for $\mathbf{4P_1}$ and **7P**, due to the steric repulsion of the nearby structures. The C−C bond length in the aromatic ring is between 1.37 and 1.46 Å, which slightly differs from the normal length, 1.40 Å, of benzene. The bond length of C_1C_2, 1.41 Å, is somewhat shorter than that of the normal single C−C bond, ∼1.45 Å, and can be attributed to the interaction between the radical on the 2p orbital of C_1 and the aromatic π orbitals. This interaction also explains the elongation of bonds C_2C_3 and C_2C_7 to be ∼1.45 Å compared to the C−C bond length in benzene. The σ-type radical center is located at the sp^2 orbital of C_6 perpendicular to the aromatic π orbital. The Coulomb repulsion near C_6 atom is weaker because of the single occupancy of this orbital, so the π electrons are drawn to stay near the atom. Consequently, the bond length of C_5C_6 and C_6C_7 is shortened to 1.38 and 1.37 Å, respectively, and the angle $\angle C_5C_6C_7$ is enlarged to 128°.

The cyclic structure also largely influences the critical bond length for enyne−butatrienes. The bond length R_{C3C8} of cyclic enyne−butatrienes **10R**, **11R**, and **12R** decreases by about 0.7, 0.5, and 0.4 Å, respectively, in comparison to that of acyclic reactants **8R** and **9R**. Other bond lengths are hardly affected by the cyclic structure. However, all bond angles that are linear in acyclic reactants are distorted. Among them, the angles $\angle C_1C_2C_3$ and $\angle C_7C_8C_b$ are distorted severely in **10P**, by about 24° and 22°, respectively. Like the angle $\angle C_1C_2C_3$ in enyne−allenes, the angle $\angle C_2C_3C_4$ in **10P**−**12P** is about 174.0°, which keeps linearity relatively well.

As the Myers−Saito cyclization proceeds, a radical will be formed in the C_2 center. For acyclic system **8** or **9**, the newly formed radical is thought to be located at the 2p orbital. And, the 2p orbital is rotated by about 90.0° to stabilize the radical; i.e., the *2*p orbital is perpendicular to the benzene ring. Nevertheless, it is another case for the cyclic systems **10**−**12**. Due to the confinement of the ring, the radicals in the products **10P**−**12P** have to be located at the sp^2 orbital of C_2 atom. This can also be seen from the angle $\angle C_1C_2C_3$, where each deviates evidently from 180°. With the enlargement of the ring, the angle $\angle C_1C_2C_3$ increases markedly to release the ring strain; the angle $\angle C_1C_2C_3$ is 116.6° in **10P**, whereas it increases to 129.7° in **11P** then to 144.8° in **12P**. Another important structural feature that should be noted is that the critical distance R_{C3C8} is 1.503 Å for **10P** and differs significantly from ∼1.45 Å of others. This is ascribed to the large ring strain of 1,5-didehydroindene **10P**. On the other hand, even more importantly vide infra, the through-bond coupling[42] between the bond C_3−C_8 and the two radicals weakens the strength of this bond.

Energies of the Myers−Saito Reaction. The zero-point corrected reaction energy and reaction barrier for the prototypical Myers−Saito cyclization **1** are −11.45 and 18.20 kcal/mol, respectively. When a methyl group is attached to the C_1 atom in reactant **1R**, i.e., **2R**, there are, as previously mentioned, two possible reaction paths as shown in Scheme 2. The barriers for both paths are calculated to be lower than that for the basic reaction **1**

SCHEME 2

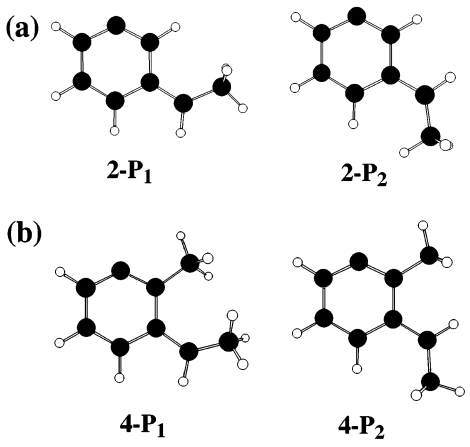

because of the hyperconjugation interaction between the radical and the nearby methyl group, and this interaction also accounts for the decrease of the reaction energies for both paths. However, when the methyl group is attached to the C_7 atom, i.e., for reaction **3**, the barrier and the reaction energy increase by 1.5 and 5.2 kcal/mol, respectively. This finding closely resembles the case in the Bergman reaction[20] where the barrier increases by 1.5 kcal/mol and the reaction energy increases by 5.2 kcal/mol. When these two methyl groups are attached simultaneously to the parent compound, the barrier increases by 2.21 kcal/mol for pathway **A** and 1.31 kcal/mol for pathway **B**. Pathway **A** is unfavorable due to the larger steric repulsion of the two methyl groups. This repulsion also disfavors the stability of the corresponding product $\mathbf{4P_1}$ and raises the reaction energy of pathway **A** by 8.41 kcal/mol in comparison to the basic reaction and it is more remarkable than the raise of pathway **B** (5.07 kcal/mol). For the nine-membered ring enyne−allene **5R**, the reaction barrier is 12.83 kcal/mol. With the enlargement of the ring, the barrier increases to 13.38 kcal/mol for the 10-membered ring enyne−allene **6R** then to 16.03 kcal/mol for the 11-membered ring enyne−allene **7R**, which is very close to those for acyclic enyne−allenes.

The cyclization barrier for the prototypical enyne−butatriene **8R** is 17.35 kcal/mol, close to that for the enyne−allene bearing the same number of carbons, **2R**, implying that the hyperconjugation interaction also exists between the vinyl group and the radical. Yet, the reaction energy is predicted to be −3.74 kcal/mol, higher than −11.96 kcal/mol for reaction **2**, and indicates clearly that the product, **8P**, is not as stable as its counterpart **2P**. The influence of the methyl group attached to the C_8 atom on the barrier and reaction energy is similar to the corresponding enyne−allene reaction **3**. In comparison to reaction **8**, the barrier and reaction energy of reaction **9** increase by 2.32 and 4.56 kcal/mol, respectively. Similarly, the ring strains lower the barriers of reactions **10**−**12** to 15.76, 13.81, and 15.83 kcal/mol, respectively, and the reaction energies to 9.28, −0.10, and 1.48 kcal/mol, respectively.

It should be noted that reaction **10** shows some particularities in energetic aspects. First, unlike the cyclic enyne−allene systems, for which the larger the ring size, the lower the barrier, the barrier of the reaction **10** is, on the contrary, higher than that of reaction **11,** which

(42) Hoffmann, R.; Imamura, A.; Hehre, W. J. *J. Am. Chem. Soc.* **1968**, *90*, 1499.

has less ring strain. On the other hand, the cyclization of **10R** is obviously an endothermic reaction, rather than an exothermic one, as most Myers−Saito reactions in the present study (the thermochemical properties of reactions **9**, **11**, and **12** seem to be ambiguous). This may be the reason **10R** is the core structure of naturally occurring antitumor drugs, whereas others have, so far, not been found to be; a detailed discussion is given in the next section.

Comparisons of the activation free energy at 298.15 K with the zero-point energy corrected reaction barrier (see Table 2) show that the difference between each other is in the range of 1.1−2.8 kcal/mol for acyclic systems, **1R**−**4R**, **8R**, and **9R**, and 0.4−0.9 kcal/mol for cyclic systems **5R**−**7R** and **10R**−**12R**. The differences for the cyclic systems are less than those for the acyclic systems. Similar results are also observed in the comparisons of the free energy of reaction (ΔG) to the reaction energy (ΔE), demonstrating that the Myers−Saito reactions for cyclic systems have fewer temperature effects. Moreover, it has been found that there is a trend, despite being not quite obvious, that the smaller the ring is the less temperature effect the corresponding reaction has. These arguments are further supported by the comparisons of the thermodynamic properties including ΔH, $\Delta H^{\ddagger}$, ΔS, $\Delta S^{\ddagger}$, ΔG, and $\Delta G^{\ddagger}$ for these reactions at different temperatures, similar to the conclusions drawn in the previous study of the Bergman reactions.[20]

Comparison with the Bergman Reaction. Reactant **10R**, (*Z*)-1-cyclononene-3,8-diyne (**13R**), and (*Z*)-1-cyclodecene-3,9- yne (**14R**) are the core structures of naturally occurring antitumor drugs. Compound **10R** conducts the Myers−Saito reaction, while **13R** and **14R** conduct the Bergman reaction. It is reasonable to believe that the similarity of reactivity may exist among these three reactions. However, it has been found both experimentally and theoretically that the prototypical Bergman reaction differs remarkably from the reaction **1** in the reaction energy. The former reaction is endothermic with ΔE 8.4 ± 3.0 kcal/mol,[43] and the latter is exothermic with ΔE −15 ± 3.0 kcal/mol.[2b] This difference can be explained well in terms of the biradical characters and stabilities of the products. The difference in reaction barrier is not so obvious as in the reaction energy, 28.23 ± 0.5 kcal/mol for prototypical Bergman reaction[43] and 21.8 ± 0.8 kcal/mol for reaction **1**.[2b]

The ring strain effect of Bergman reactions and Myers−Saito reactions of enyne−allene type, despite being significant, does not change the biradical character of the products. But, for the Myers−Saito reactions of the enyne−butatriene type, the presence of the ring forces one of the newly formed single-electron to be located at the sp^2 orbital of C_2; i.e., it leads to an essential transformation of the biradical character from the $\sigma-\pi$ type to the $\sigma-\sigma$ type. Therefore, the Myers−Saito products of cyclic enyne−butatrienes **10P**−**12P**, despite benefiting from the through-bond coupling, are predicted to be not as stable as those of cyclic enyne−allenes **5P**−**7P**. This is shown clearly in Table 2, in which the reaction energies of systems **10**−**12** are higher than those of the cyclic enyne−allene systems **5**−**7**.

(43) (a) Lindh, R.; Lee, T. J.; Bernhardsson, A.; Persson, B. J.; Karlstrom, G. *J. Am. Chem. Soc.* **1995**, *117*, 7186. (b) Roth, W. R.; Hopf, H.; Horn, C. *Chem. Ber.* **1994**, *127*, 1765.

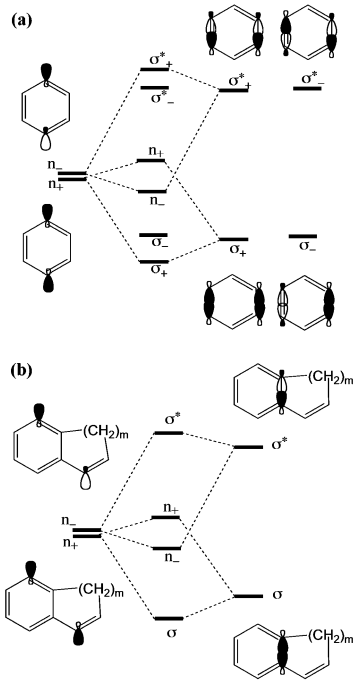

FIGURE 2. Through-bond coupling in (a) 1,4-didehydrobenzene and (b) 1,5-didehydroindene (**10P**).

Unlike in the Bergman products, the through-bond coupling in **10P**, as depicted in Figure 2, involves only one σ bond (C_3-C_8). Due to orbital interaction, there are two electrons to be filled in the n_ orbital that have been mixed with the σ^* component. Therefore, the through bond coupling weakens the σ bonding of C_3-C_8, and accordingly, increases the bond length. As the ring size increases, the ring strains decrease rapidly. To benefit from the benzylic stabilization instead of the weaker through bond coupling, the orbital that the C_2 radical center located must be approximately perpendicular to the benzene ring. Hence, the product has a tendency to increase the angle $\angle C_1C_2C_3$ facilitating the bond C_2-C_3 to rotate more freely. In turn, these geometrical changes lower the overlap between the interacting orbitals and weaken the through-bond coupling. As a consequence, **10P** represents a particularly long critical distance (R_{C3C8}) and lower thermodynamic stability, compared to other cyclic enyne−butatriene products. Furthermore, the Myers−Saito cyclization is characteristic of a late transition state; i.e., the transition state **10TS** resembles the product **10P** in structure and energy more closely than the reactant **10R**. Thus, it seems reasonable that the energy of the corresponding transition state **10TS** is also higher than expected, so the barrier of reaction **10** is out of the trend.

Comparing the structures related to reactions **10**, **13**, and **14**, we found that the critical distances, whether in reactant, transition state, or product, are very close. Also found to be close are the imaginary frequencies of the corresponding transition structures, which are 469i for **10TS**, 446i for **13TS**, and 450i for **14TS**, respectively. Figure 3 gives the relationships of energy profiles for these three reactions established through the complete IRC calculations. As seen from Figure 3, the curvature of the three reaction paths is very similar, and the

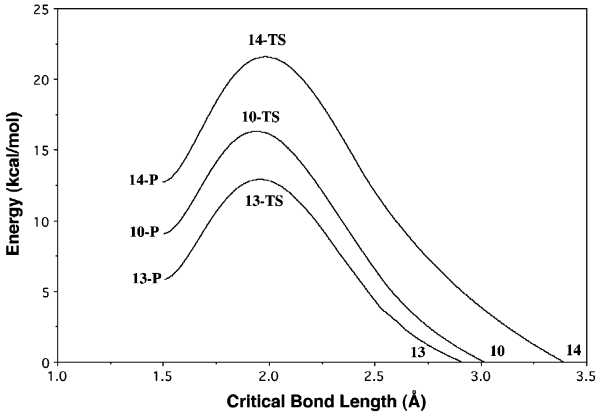

FIGURE 3. Energetic profiles of the Myers−Saito reaction **10** and Bergman reactions **13** and **14**.

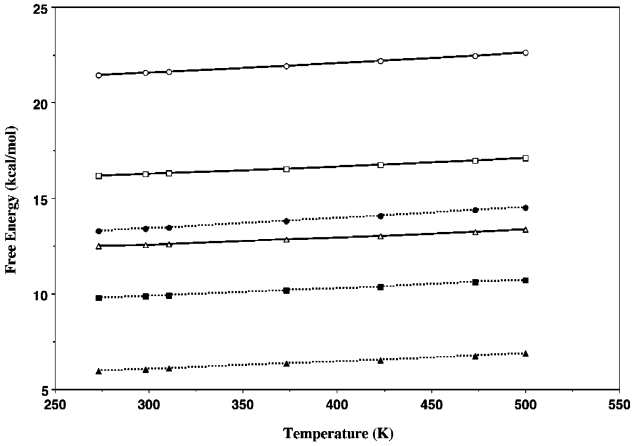

FIGURE 4. Free energy (ΔG) and activation free energy ($\Delta G^{\ddagger}$) plotted against temperature (T) for Myers−Saito reaction **10** (square) and Bergman reactions **13** (triangle) and **14** (circle). The solid lines correspond to the plots of $\Delta G^{\ddagger}$ vs T, and the dashed lines correspond to the plots of ΔG vs T.

reaction path of **10** is shown definitely to lie between that of **13** and **14**. Thus, the reactivity of these three reactions is expected to be quite similar. Additionally, compared to previously calculated thermodynamic properties for reaction **13** and **14**, all the quantities including ΔG, $\Delta G^{\ddagger}$, ΔH, $\Delta H^{\ddagger}$, ΔS, and $\Delta S^{\ddagger}$ at different temperatures for the reaction **10** are also found to lie between those for reactions **13** and **14**. In Figure 4 are plotted the ΔG and $\Delta G^{\ddagger}$ at 273.17−500 K for these three reactions. If one slides the curves of activation free energy ($\Delta G^{\ddagger}$) against temperature downward, these curves can be found to coincide well with those of free energy (ΔG) against temperature. This suggests that the reverse activation free energies for these reactions are close to one another; therefore, the products **10P**, **13P**, and **14P** have similar stabilities with respect to the reverse Myers−Saito or Bergman reaction, which is consistent with our previous speculation.[20] Since the reverse Myers-Saito or Bergman reaction may compete with the H-abstraction reaction of the biradical product, the reverse activation free energies are of particular importance for designing new enediyne antitumor drugs.[17a]

Although the activation free energies for other enyne−allenes and enyne−butatrienes at normal physiological temperature (310 K) are within the range of 13.23−23.31 kcal/mol and most of them are lower than the reference value (22 kcal/mol) proposed by Kraka et al.,[17a] only **10R** is found in naturally occurring antitumor drugs. This is probably because all other reactions are exothermic. According to thermodynamic principle, spontaneous cyclizations for these corresponding reactants take place easier than those of **10R**. Therefore, an early H-abstraction reaction may take place for these reactants before docking to the target site in a tumor cell and leads to loss of antitumor activity.

Conclusions

In the present work, the prototypical Myers−Saito reaction **1** is examined by using different methods. We found that the pure DFT method, BPW91, which was selected in a previous study of Bergman cyclizations, reproduces well the experimental and high-level ab initio calculated reaction barrier and reaction energy and is suitable to study the Myers−Saito cyclization.

A detailed comparison of geometrical parameters for the systems considered in the present work shows that the cyclic structures, as found in Bergman reactions, reduce the critical distances of reactants (R_{C2C7} in enyne-allenes or R_{C3C8} in enyne−trienes) substantially. As Myers−Saito cyclization proceeds, the newly formed radical in the C_2 site has a tendency to be located at the 2p orbital, to obtain benzylic stabilizations. Thus, in most cases, the Myers−Saito products are σ−σ-type biradicals, as **1P**−**9P** represent. However, the products of the cyclic enyne−triene, **10P**, are found to be a σ−σ type biradical because the confinement of the ring forces the radical in the C_2 site to be located at the sp^2 orbital instead of the 2p orbital. Similar to Bergman products, **10P** also involves the through-bond coupling between the two single electrons. With the enlargement of the ring, the angle $\angle C_1C_2C_3$ increases markedly in order to benefit from the benzylic stabilization rather than the weaker through-bond coupling, which in turn disfavors the through-bond coupling. Hence, **10P** possesses a particularly long critical distance (R_{C3C8}) and smaller thermodynamic stability compared to other Myers−Saito products.

The calculations of thermodynamic properties for reactions **1**−**12** reveal that the influence of temperature on the reactivity of the Myers−Saito cyclization is rather limited. Moreover, the temperature effects for the cyclic systems are generally less than those for acyclic systems, and the smaller the ring, the less temperature effect the corresponding reaction.

In view of the reactant **10R**, as well as previously studied Bergman reactants **13R** and **14R** representing the core structures of naturally occurring antitumor drugs, a detailed comparison of these three systems have been made. The prototypical Myers−Saito reaction, reaction **1**, is exothermic while Bergman reaction is endothermic. Although Myers-Saito and Bergman reactions differ remarkably in reaction enthalpy, the reactivity of the systems **10**, **13**, and **14** is quite similar, whether being judged from free energy ΔG and activation free energy

$\Delta G^{\ddagger}$, or from other thermodynamic properties such as ΔH, $\Delta H^{\ddagger}$, ΔS, and $\Delta S^{\ddagger}$. This demonstrates that the ring modification plays an important role in these systems.

Acknowledgment. We acknowledge support from the National Science Council of the Republic of China under Grant No. NSC 91-2113-M-007-034.

Supporting Information Available: Tables of optimized geometrical parameters for **1R**−**12R**, **1P**−**12P**, and **1TS**−**12TS** (Tables S1−S6) and the thermodynamic data not listed in Table 2 (Table S7). The BPW91/6-311G**-optimized Cartesian coordinates and total energies for all species. This material is available free of charge via the Internet at http://pubs.acs.org.

JO0267246